Journal of Neurochemistry

JNC

JOURNAL OF NEUROCHEMISTRY | 2019

doi: 10.1111/jnc.14654

ORIGINAL ARTICLE

The dependence of brain mitochondria reactive oxygen species production on oxygen level is linear, except when inhibited by antimycin A

Anna Stepanova*†, Csaba Konrad‡, Giovanni Manfredi‡, Roger Springett§, Vadim Ten† and Alexander Galkin*†

*Queen's University Belfast, School of Biological Sciences, Medical Biology Centre, Belfast, UK

†Department of Pediatrics, Columbia University, New York, NY, USA

‡Feil Family Brain and Mind Research Institute, Weill Cornell Medicine, New York, NY, USA

§Cardiovascular Division, King's College London, British Heart Foundation Centre of Excellence London, London, UK

Abstract

Reactive oxygen species (ROS) are by-products of physiological mitochondrial metabolism that are involved in several cellular signaling pathways as well as tissue injury and pathophysiological processes, including brain ischemia/reperfusion injury. The mitochondrial respiratory chain is considered a major source of ROS; however, there is little agreement on how ROS release depends on oxygen concentration. The rate of H_2O_2 release by intact brain mitochondria was measured with an Amplex UltraRed assay using a high-resolution respirometer (Oroboros) equipped with a fluorescent optical module and a system of controlled gas flow for varying the oxygen concentration. Three types of substrates were used: malate and pyruvate, succinate and glutamate, succinate alone or glycerol 3-phosphate. For the first time we determined that, with any substrate used in the absence of inhibitors, H_2O_2 release by respiring brain mitochondria is linearly dependent on the oxygen concentration. We found that the highest rate of H_2O_2 release occurs in conditions of reverse electron transfer when mitochondria oxidize succinate or glycerol 3-phosphate. H_2O_2 production by complex III is significant only in the presence of antimycin A and, in this case, the oxygen dependence manifested mixed (linear and hyperbolic) kinetics. We also demonstrated that complex II in brain mitochondria could contribute to ROS generation even in the absence of its substrate succinate when the quinone pool is reduced by glycerol 3-phosphate. Our results underscore the critical importance of reverse electron transfer in the brain, where a significant amount of succinate can be accumulated during ischemia providing a backflow of electrons to complex I at the early stages of reperfusion. Our study also demonstrates that ROS generation in brain mitochondria is lower under hypoxic conditions than in normoxia.

Keywords: antimycin A, complex I, ischemia/reperfusion, mitochondria, reverse electron transfer, ROS generation.

J. Neurochem. (2018) https://doi.org/10.1111/jnc.14654

The major energy-generating metabolic pathway in most mammalian cells is oxidative phosphorylation, where molecular oxygen is reduced to water by the mitochondrial respiratory chain. As a by-product, mitochondria are also able to catalyze the one-electron reduction in oxygen to produce the superoxide radical ($O_2^{\cdot -}$), a precursor of hydrogen peroxide (H_2O_2), which is the most common reactive oxygen species (ROS) in the cell (Loschen *et al.* 1974; Murphy 2009; Andreyev *et al.* 2015). Therefore, ROS formation is an inherent property of aerobic mitochondrial metabolism catalyzed by the respiratory chain complexes and matrix enzymes (Andreyev *et al.* 2005). The processes leading to the generation of ROS have gained significant attention over the last 30 years because of their involvement in apoptosis, hypoxic cellular responses, aging, and various signaling pathways [reviewed in (D'Autreaux and Toledano

Received March 2, 2018; revised manuscript received May 11, 2018, December 10, 2018; accepted December 14, 2018.

Address correspondence and reprint requests to Alexander Galkin, Pediatrics Department, Columbia New York, NY 10032, USA. E-mail: ag4003@cumc.columbia.edu

Abbreviations used: FAD, flavin adenine dinucleotide; FMN, flavin mononucleotide; GDPH, glycerol 3-phosphate dehydrogenase; RET, reverse electron transfer; ROS, reactive oxygen species.

2007; Schieber and Chandel 2014)]. Mitochondria are commonly considered a major source of ROS, but the conditions under which mitochondrial ROS are produced are still a matter of debate (Starkov *et al.* 2014).

Excessive levels of ROS lead to oxidative stress, which plays a crucial role in mediating tissue damage after brain ischemia/reperfusion (Lust *et al.* 2002; Kalogeris *et al.* 2014). Brain tissue is specifically vulnerable to the deleterious effects of oxidative stress because of its low capacity for cell division and repair. Since molecular oxygen is also the substrate of ROS generation, the dependence of this reaction on oxygen concentration has been studied by several groups, but mostly in hyperoxic/hyperbaric conditions, using mitochondria from liver and heart (Boveris *et al.* 1972; Boveris and Chance 1973; Oshino *et al.* 1975; Turrens *et al.* 1982a,b). Until now, the relationship between oxygen concentration and ROS production has never been carefully analyzed in intact brain mitochondria. This knowledge is of great importance for brain ischemia/reperfusion studies where the interplay between energy failure, oxygen availability, and ROS generation is critical. To our knowledge, the effect of oxygen concentration on the rate of H_2O_2 release by intact brain mitochondria has only been analyzed under limited experimental settings and only at supraphysiological oxygen concentrations (Kudin *et al.* 2004).

Here, we performed a systematic analysis of H_2O_2 release from intact mouse brain mitochondria and demonstrate that, under normal respiration, the release of H_2O_2 is directly proportional to oxygen concentration regardless of the respiratory substrates used. The highest rates of H_2O_2 release were registered under conditions of reverse electron transfer (RET). Our data also demonstrate that complex III is not a major contributor to ROS generation in physiological conditions. Antimycin A significantly stimulates complex III ROS production, and its oxygen dependence manifests Michaelis–Menten-like kinetics. We also found that, even in the absence of succinate, complex II can contribute to ROS generation when the quinone pool is reduced by glycerol 3-phosphate.

Materials and methods

Sources of chemicals, animal, and mitochondria

The study was not preregistered, and all experiments were performed *in vitro* using intact mouse brain mitochondria; no blinding was required. Most of the chemicals were purchased from Sigma, including fatty acid free bovine serum albumin (Cat# A6003), glycerol 3-phosphate (Cat# 50019), rotenone (Cat# R8875), antimycin A (Cat# A8674), and myxothiazol (Cat#T5580). Pierce BCA protein assay kit (Cat# 23225), Amplex UltraRed (Cat# A36006), and horseradish peroxidase (Cat# 012001) were from Thermo Fisher Scientific. Atpenin A5 was from Cayman Chemical (Cat# 11898). All procedures were approved by the Institutional Animal Care and Use Committee of Weill Cornell Medicine and performed in accordance with the ARRIVE guidelines (Kilkenny *et al.* 2010). Intact mitochondria were isolated from 8 to 10 weeks C57Bl/6 male mice ((IMSR Cat# JAX:000664, RRID: IMSR_JAX:000664) by differential centrifugation with digitonin treatment (Rosenthal *et al.* 1987; Stepanova *et al.* 2017). The forebrain hemispheres were excised and immediately immersed into ice-cold isolation medium (225 mM mannitol, 75 mM sucrose, 20 mM HEPES-Tris, 1 mM EGTA, 1 mg/mL bovine serum albumin (BSA), pH 7.4). The tissue was homogenized with 40 strokes of a Dounce homogenizer with a tight pestle in 10 ml of the isolation medium, diluted twofold, and centrifuged at 5900 g for 4 min in a Beckman centrifuge at 4°C. The supernatant was supplemented by 0.02% digitonin and centrifuged again at 10 000 g for 10 min. The pellet was then gently resuspended in the isolation buffer without BSA and washed twice by centrifuging at 10 000 g for 10 min. The mitochondrial pellet was then resuspended in 0.15 mL of washing buffer and stored on ice.

Assessing respiration and H_2O_2 production in intact mitochondria

A high-resolution respirometer (O2k, Oroboros Instruments GmbH) was equipped with homebuilt two-channel fluorescence optical module to monitor simultaneously oxygen concentration and H_2O_2 production as described in detail (Stepanova *et al.* 2017) with a data collection interval of 0.2 s. H_2O_2 release was measured from the fluorescence of resorufin formed from Amplex UltraRed reacting with H_2O_2 in the presence of horseradish peroxidase. The fluorescence was calibrated into an H_2O_2 concentration by addition of 90 nM of H_2O_2 to the chamber at the end of the study. To change oxygen levels, humidified pre-purified argon gas was equilibrated with the media of the respirometer chamber at a flow rate of 10–60 mL/min. For effective gas exchange, a custom stopper for the Oroboros chamber was built that created 1 mL gas headspace above the liquid phase and contained two channels for probes. This system allows the monitoring of oxygen concentration but not mitochondrial respiration because of exchange of oxygen between the medium and the head space.

Mitochondria (0.1–0.5 mg/mL) were added to assay media containing 125 mM KCl, 14 mM NaCl, 0.2 mM EGTA, 4 mM KH_2PO_4, 2 mM $MgCl_2$, 20 mM HEPES-Tris, pH 7.4, supplemented with 2 mg/mL BSA, 10 μM Amplex UltraRed reagent, 4 U/mL horseradish peroxidase, and 40 U/mL Cu/Zn superoxide dismutase at 37°C. No change in fluorescent signal was observed in the presence of 100 U/mL catalase. Three different substrate combinations were tested: 2 mM malate and 5 mM pyruvate, 5 mM succinate and 1 mM glutamate, and 5–40 mM glycerol-3-phosphate. The concentration of glycerol 3-phosphate was 40 mM if not specified otherwise. For each substrate combination, three different experimental conditions were used: non-phosphorylating respiration (resting respiration, substrates are present, ADP is absent), state 3 phosphorylating respiration (ADP-stimulated respiration, substrates, and 200 μM ADP present), and inhibited respiration (substrates and inhibitor are present, ADP is absent).

The combination of malate and pyruvate was used to generate matrix NADH for respiration by complexes I-II-IV. Here, the pyruvate is oxidized by pyruvate dehydrogenase generating NADH and acetyl-CoA which further reacts with matrix oxaloacetate to shift the malate dehydrogenase reaction toward oxidation of malate and formation of NADH. succinate and glutamate couple provide respiration via complexes II-III-IV. The succinate is the direct

substrate of complex II and glutamate is used by glutamic-oxaloacetic transaminase to remove oxaloacetate, a potent inhibitor of complex II. Glycerol 3-phosphate is a substrate of mitochondrial glycerol 3-phosphate dehydrogenase (GPDH) located on the outer surface of the inner mitochondrial membrane which uses quinone as an electron acceptor providing electron transfer toward complexes III-IV (Patole *et al.* 1986; Kwong and Sohal 1998).

Data analysis and curve fitting

All data calculations were performed using R (version 3.5.1) in RStudio (Version 1.1.456, Boston, MA, USA). The rate of H_2O_2 release was calculated by differentiation of the total H_2O_2 released using the Package *locfit* which simultaneously performs smoothing and differentiation of the graph data by applying a local quadric fitting with a bandwidth of 10–20 data points (other parameters were kept at default). At least five separate preparations of mitochondria were used for each experimental condition. To generate the final dataset of H_2O_2 rate at different oxygen concentrations, at least 5–8 traces for each experimental condition were averaged using adjusted oxygen concentrations. The averaged curves of H_2O_2 release rate versus oxygen concentration were fitted either using a linear function (Equation 1) or a sum of linear and hyperbolic functions (Equation 2) (Fig. 1e, f):

$$y = k \cdot x + \text{const} \quad (1)$$

$$y = \frac{a \cdot x}{k_m + x} + k \cdot x + \text{const} \quad (2)$$

where y is the rate of H_2O_2 release, x is the oxygen concentration, and k, a, K_m, and const are fit parameters. The details of the fitting methods can be found in the Supplement section. For clarity, only values of k and K_m are shown in the figures.

All results were expressed as means ± SEM. For fit parameters, standard errors were obtained in the weighted fitting procedure. Rates of H_2O_2 release were compared using ANOVA followed by *post hoc* pair-wise *t*-tests with false discovery rate correction for multiple comparisons. Normality of data was assessed using three tests: Shapiro–Wilk, Anderson–Darling, and Kolmogorov–Smirnov. Chi-squared test for outliers was conducted. Other experimental details are described in the figure legends.

Results

Rates of H_2O_2 release by brain mitochondria at ambient oxygen concentration depend on respiratory substrates and the presence of respiratory chain inhibitors

Our goal was to investigate the effect of physiologically relevant oxygen concentrations on ROS production in intact brain mitochondria. First, we determined the rates of H_2O_2 release from mitochondria respiring at ambient oxygen (200 μM [O_2]) with different combinations of substrates. Rates of oxygen consumption and H_2O_2 release by intact brain mitochondria oxidizing malate and pyruvate, succinate and glutamate or succinate, and glycerol 3-phosphate alone are summarized in Table 1. For each of three substrates combinations, we measured H_2O_2 release in different respiratory states as well as in the presence of two specific respiratory chain inhibitors, rotenone and antimycin

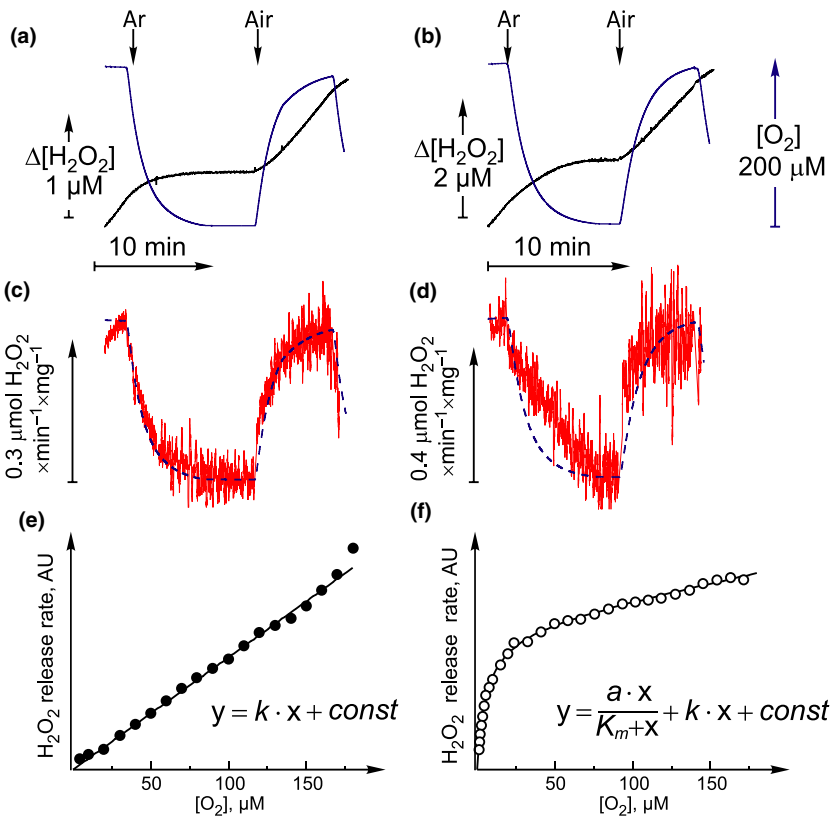

Fig. 1 Scheme of assessment of the effect of oxygen concentration on H_2O_2 release by intact mitochondria in different conditions. The reaction started with the addition of mitochondria (0.5 mg protein/mL) to the assay media containing 5 mM succinate and 1 mM glutamate (left panel) or 10 mM glycerol 3-phosphate and 1 μM antimycin A (right panel). Oxygen concentration as measured directly by the Oroboros respirometer was rapidly varied by continuously purging the headspace with argon (Ar) or air as detailed in the Materials and Methods section. (a and b) Representative registration traces of oxygen concentration (blue) and release of H_2O_2 measured with Amplex UltraRed (black). (c and d) The calculated rates of H_2O_2 release are shown as red traces. (e and f) H_2O_2 release rate versus oxygen concentration was plotted and fitted with either a linear function (e, data from (a)) or a sum of both linear and hyperbolic functions (f, data from b). Corresponding equations are shown on the graphs.

A. The highest rate of H_2O_2 release was observed in conditions of reverse electron transfer (RET) when the mitochondria have a high proton-motive force and oxidize succinate (with or without glutamate) or glycerol 3-phosphate (*t*-test, $p < 0.05$, when compared to malate and pyruvate). During this process, the proton motive force drives complex I in reverse transferring electrons from the ubiquinol pool (generated from the complex II or GPDH substrates) to reduce NAD^+. H_2O_2 release in RET was highly sensitive to the presence of ADP, which decreases the proton-motive force, or the complex I specific inhibitor rotenone, indicating that ROS release is at the level of complex I because of the RET.

Addition of the complex III inhibitor antimycin A to mitochondria affected the rate of H_2O_2 release differently depending on the substrate used. Three distinct outcomes were observed. When malate and pyruvate were used as substrates, the rate of H_2O_2 release increased, whereas with succinate and glutamate, the rate decreased. No change was observed when glycerol 3-phosphate was used as the substrate. An exceptionally high rate of ROS production was found during oxidation of glycerol 3-phosphate in the presence of antimycin A, pointing to the existence of an additional contributor to overall ROS production, besides complex III.

Oxygen concentration affects H_2O_2 release by intact brain mitochondria

To assess the effect of oxygen concentration on H_2O_2 release, we implemented the experimental approach detailed below. Fig. 1 shows representative traces of the fluorescence signal of Amplex UltraRed (Fig. 1a and b, black traces) when oxygen concentration in the medium of respiring mitochondria was rapidly changed (Fig. 1a and b, blue traces). The fluorescence signal, which is proportional to the total H_2O_2 released, was differentiated with respect to time to give the rate of H_2O_2 release (red traces, Fig. 1c and d). Variation in oxygen concentration (from 0 to 200 μM) strongly affected the rate of H_2O_2 release. We observed two different patterns of H_2O_2 release rates in response to changing oxygen concentration. In the absence of antimycin (Fig. 1c), H_2O_2 release rate (red trace) and oxygen concentration (blue dashed line) followed the same pattern whereas, in the presence of antimycin A (Fig. 1d), the trace of H_2O_2 release rate deviated from the trace of oxygen concentration.

The recorded rate of H_2O_2 release was then plotted against oxygen concentration and fitted to the mathematical function (Fig. 1e and f). In the absence of antimycin A, we observed a linear dependence of H_2O_2 release rate on oxygen concentration (Fig. 1e), while the addition of antimycin A resulted in a nonlinear curve that can be described as a sum of linear and hyperbolic functions (Fig. 1f).

H_2O_2 release by intact brain mitochondria linearly depends on oxygen concentration

We measured the oxygen dependence of H_2O_2 release by intact mitochondria oxidizing different substrates in the absence of any inhibitors of the respiratory chain. In non-phosphorylating respiring mitochondria, the H_2O_2 release rate was linearly proportional to the oxygen concentration up to 200 μM for all substrates (Fig. 2a–c, open squares). The highest rate of H_2O_2 release was recorded in conditions of RET when mitochondria oxidize succinate in the presence of glutamate (Fig. 2b). Addition of ADP to respiring mitochondria stimulated oxidative phosphorylation (state 3), decreased proton-motive force (data not shown), and strongly diminished the rates of H_2O_2 release for all substrates. The

Table 1 Respiration and H_2O_2 emission in mouse brain mitochondria

	Substrates			
Conditions	Mal/Pyr	Succ/Glu	G3P	Succ
H_2O_2 release, pmol/min/mg protein				
Non-phosphorylating (no ADP)	143 ± 14*	1748 ± 99*	1308 ± 78*	1137 ± 86
State 3 (+0.2 mM ADP)	55 ± 5*	142 ± 12	124 ± 15	134 ± 11
1 μM AntA	713 ± 56	519.0 ± 32.6	1206 ± 38*	441 ± 16
1–2 μM Rot	302 ± 17*	584.5 ± 8.4	505 ± 17	227 ± 12
1 μM Rot + 1 mM Malonate			406 ± 36	
Respiration, nmol/min/mg protein				
Non-phosphorylating (no ADP)	15.2 ± 1	52.0 ± 3.5	29.1 ± 1.9	48.7 ± 2.3
State 3 (+0.2 mM ADP)	140.2 ± 6.7	242.4 ± 15.6	82.5 ± 5.1	186.8 ± 9.4
1 μM AntA	6.2 ± 0.3	7.4 ± 0.7	3.2 ± 0.2	6.7 ± 0.5
RCR	9.5 ± 0.8	4.7 ± 0.2	2.9 ± 0.2	3.8 ± 0.3

Mal/Pyr: 2 mM malate + 5 mM pyruvate, Succ/Glu: 5 mM succinate + 1 mM glutamate, G3P: 40 mM glycerol 3-phosphate, Succ: 10 mM Succinate
AntA: antimycin A; Rot: rotenone; RCR: respiratory control ratio determined by the rate of state 3 respiration divided by the rate of non-phosphorylating respiration. (*) – mean of the group is significantly different ($p < 0.05$) from the other substrates for the same conditions.

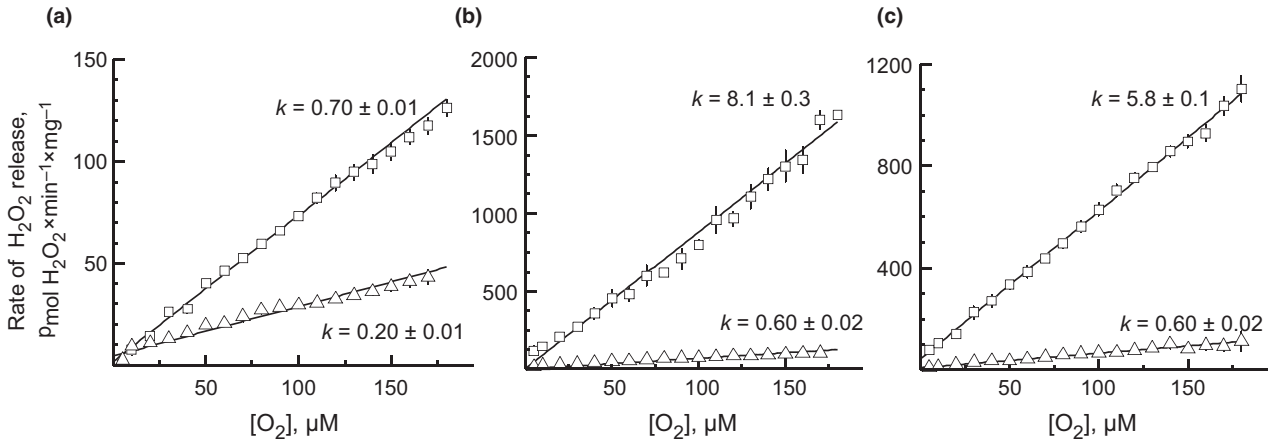

Fig. 2 Dependence of H_2O_2 release rate on the oxygen concentration in the absence of inhibitors. H_2O_2 release during non-phosphorylating (no ADP, open squares) and phosphorylating state 3 (0.2 mM ADP added, open triangles) respiration was measured at different $[O_2]$ as detailed in the Materials and Methods section. Mitochondria (0.1–0.5 mg protein/mL) were added to the assay media containing the following substrates: 2 mM malate and 5 mM pyruvate (a), 5 mM succinate and 1 mM glutamate (b), and 40 mM glycerol 3-phosphate (c). At least five different isolations of mitochondria were used and 5–6 traces for each experimental condition were averaged (n = 5–6). Fit parameters of Equation 1 are shown on the graphs.

residual H_2O_2 release in the presence of ADP was only 10% of the RET-supported ROS production (Fig. 1b and c). The linear dependence of H_2O_2 release on oxygen concentration, however, remained (Fig. 2a–c, open triangles).

Antimycin A, but not rotenone, introduces nonlinearity to the oxygen dependence of the H_2O_2 release rate

We then tested the effects of two classical inhibitors of complexes I and III—rotenone and antimycin A, respectively – on H_2O_2 release rate at different oxygen concentrations. Addition of rotenone to mitochondria increased H_2O_2 release when respiring on malate and pyruvate and decreased it in conditions of RET (Table 1, Fig. 3a–c, solid triangles). In all these conditions, the linear oxygen dependences were preserved. Surprisingly, with all substrates, in the presence of antimycin A, the oxygen dependence of H_2O_2 release displayed more complex kinetics (Fig. 3a–c, solid squares). The function of oxygen dependence under these conditions is described as a sum of linear and hyperbolic terms by Equation 2.

For malate and pyruvate-based respiration, the quantitative analysis of the fitting curve (Fig. 3a, solid squares) shows that the addition of antimycin A results in the appearance of the hyperbolic component with an apparent K_m for oxygen of 12.7 ± 0.4 μM. These results seem to indicate that, in the presence of antimycin A, ROS generation at complex III manifests itself with classical Michaelis–Menten kinetics for oxygen. At the same time, the linear term of the Equation 2 quantitatively corresponded to the slope in the presence of rotenone (Fig. 3a, triangles, 1.3 ± 0.1 pmol H_2O_2/min/mg protein per μM $[O_2]$).

For succinate and glutamate-based respiration (Fig. 3b, solid squares), the addition of antimycin A gave rise to the hyperbolic component with an apparent K_m of 6.9 ± 0.4 μM $[O_2]$. The linear term (with the slope of 1.00 ± 0.01 pmol H_2O_2/min/mg protein per μM $[O_2]$) corresponded to the rate during respiration in state 3 (Fig. 2b, open triangles, 0.60 ± 0.02 pmol H_2O_2/min/mg protein per μM $[O_2]$). Therefore, in the presence of antimycin A, the hyperbolic dependence originates from complex III while the linear component is provided by the activity of the respiratory chain operating in the absence of a proton-motive force upstream of the block imposed by the inhibitor.

For glycerol 3-phosphate-based respiration, the addition of antimycin A also resulted in a mixed hyperbolic and linear dependence pattern (Fig. 3c, solid squares). The apparent K_m value for the first component was 5.9 ± 0.3 μM $[O_2]$. The slope of the linear term was 2.2 ± 0.1 pmol H_2O_2/min/mg protein per μM $[O_2]$, most likely corresponding to the production of ROS by the enzymes upstream of the antimycin A block in the absence of proton-motive force.

Oxidation of glycerol 3-phosphate and H_2O_2 release

As shown previously, mitochondrial GPDH located on the outer surface of the inner mitochondrial membrane can generate ROS at a significant rate (Patole *et al.* 1986; Kwong and Sohal 1998; Miwa *et al.* 2003; Tretter *et al.* 2007). Activity of GPDH is strongly dependent on the concentration of the substrate (Tretter *et al.* 2007; Orr *et al.* 2012). We also found that both oxidation of glycerol 3-phosphate (Fig. 4a) and H_2O_2 release (Fig. 4b) depended on the concentration of the substrate in the millimolar range.

We tested the effect of complex II inhibition on the rate of H_2O_2 release when mitochondria are oxidizing glycerol 3-phosphate. These experiments were carried out in the

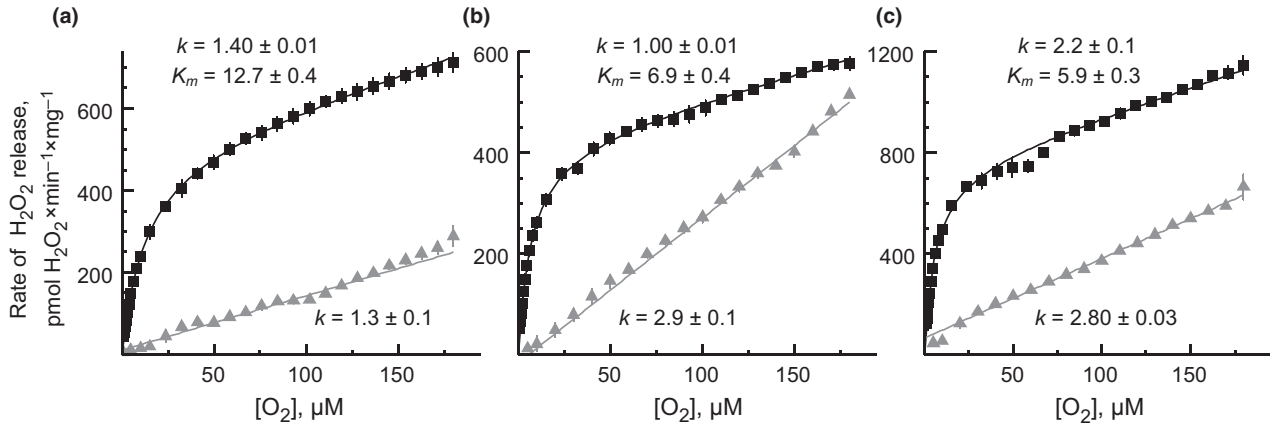

Fig. 3 Dependence of H_2O_2 release rate on the oxygen concentration for mitochondria in the presence of respiratory chain inhibitors. Experimental conditions were the same as in Fig. 2. with the following substrates 2 mM malate and 5 mM pyruvate (a), 5 mM succinate and 1 mM glutamate (b), or 40 mM glycerol 3-phosphate (c). No ADP was present. The H_2O_2 release at different $[O_2]$ in the presence of 1 μM rotenone (solid triangles) or 1 μM antimycin A (solid squares) was measured as described in the Materials and Methods. At least five different isolations of mitochondria were used and 5–9 traces for each experimental condition were averaged (n = 5–9). Fit parameters of Equations 1 and 2 are shown on the graphs.

presence of rotenone to prevent RET-induced H_2O_2 release, and we used atpenin A5, a potent inhibitor of complex II, to block electron transfer at the ubiquinone-binding site of the enzyme (Miyadera *et al.* 2003; Horsefield *et al.* 2006). In all tested conditions, the rate of H_2O_2 release was decreased by the addition of atpenin (Fig 4c–e). The effect of complex II inhibition was less pronounced when the mitochondrial membrane potential was collapsed with an uncoupler (Fig. 5d) and more pronounced when quinone pool was fully reduced by inhibiting complex III with myxothiazol (Fig. 4e). Complex II contribution calculated from an atpenin-sensitive fraction of total H_2O_2 release was around 21% during non-phosphorylating respiration (Fig. 4c), and the addition of uncoupler decreased it to only 17% (Fig. 4d). In the presence of myxothiazol, complex II contribution was half of the total H_2O_2 release rate. Therefore, in isolated brain mitochondria, complex II can contribute to overall H_2O_2 release, even in the absence of succinate.

Discussion

It is generally accepted that mitochondria are key organelles involved in ROS metabolism, both as producers and scavengers of ROS (Starkov *et al.* 2014; Andreyev *et al.* 2015). The relationship between ROS generation by mitochondria and oxygen concentration has been the subject of controversy in the recent literature. After the pioneering work from the Chance lab (Boveris and Chance 1973), it was accepted that hyperbaric oxygen stimulates H_2O_2 production. The H_2O_2 release rate by heart intact mitochondria was found to almost linearly correlate with oxygen concentration, between 1 and 10 atmospheric pressure of oxygen (Boveris and Chance 1973). The effect of oxygen concentration on H_2O_2 release by perfused liver was later revisited in the same laboratory (Oshino *et al.* 1975), and it was concluded that H_2O_2 production increases with increasing oxygen concentration, within physiological intervals of $[O_2]$. However, only 10–15% of H_2O_2 production in the liver can be attributed to mitochondria (Boveris *et al.* 1972). H_2O_2 release by intact lung mitochondria, as well as superoxide production during NADH oxidation by lung submitochondrial particles in the presence of inhibitors, was also directly correlated with oxygen concentration in hyperoxic (200–800 μM $[O_2]$) conditions (Turrens *et al.* 1982a,b). More recently, H_2O_2 production dependence on oxygen concentrations was tested using rat brain mitochondria at very high oxygen level (200–1000 μM $[O_2]$) (Kudin *et al.* 2004). The authors suggested hyperbolic concentration dependences with an apparent K_m for oxygen of approximately 1 mM for mitochondria oxidizing either malate/glutamate or succinate, while the experimental data fitted well to a linear dependence.

In this study, we showed for the first time that H_2O_2 release by intact brain mitochondria in the absence of inhibitors depends linearly on oxygen concentration in the physiological range (<200 μM $[O_2]$). This included non-phosphorylating (resting) and phosphorylating (state 3) respiration during forward electron transfer from the substrates of NAD-dependent dehydrogenases (malate and pyruvate) as well as in RET-like conditions during oxidation of succinate or glycerol 3-phosphate. We conclude that, in the absence of inhibitors, there is no specific site for oxygen binding in the reaction of mitochondrial ROS formation and this process obeys pseudo-first-order kinetics and can be considered as an electron "leak" from the reduced redox center(s) of the respiratory chain. Our finding agrees with recent observations of linear dependence of superoxide generation by mammalian

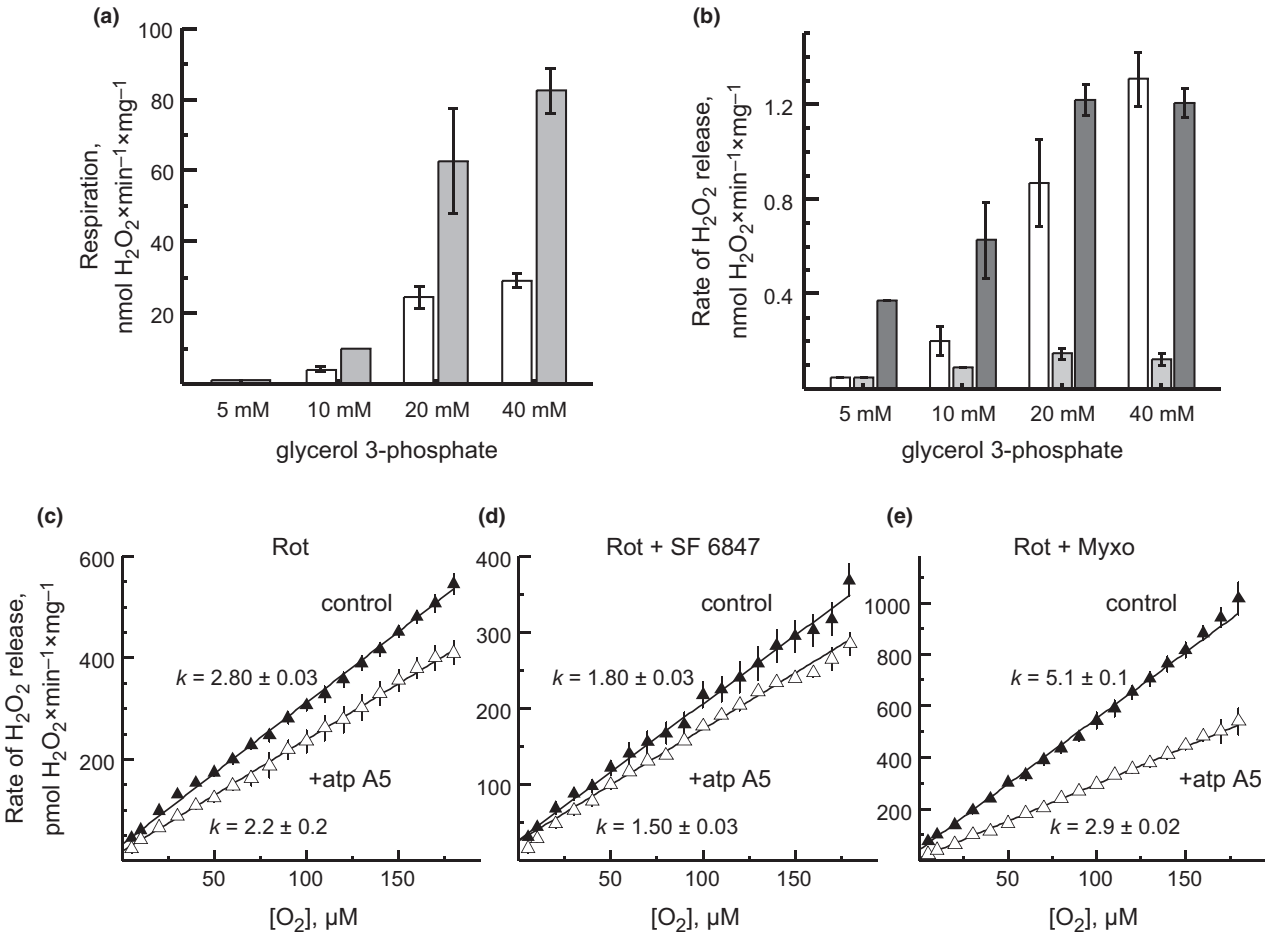

Fig. 4 Respiration and H_2O_2 release by mitochondria oxidizing glycerol 3-phosphate. (a) Effect of glycerol 3-phosphate concentration on non-phosphorylating (no ADP added, white bars) and state 3 phosphorylating respiration (0.2 mM ADP, gray bars). (b) Effect of glycerol 3-phosphate concentration on non-phosphorylating H_2O_2 release (white bars), state 3 phosphorylating H_2O_2 release (gray bars), and antimycin A-inhibited H_2O_2 release (black). (c–e) Effect of complex II-specific inhibitor atpenin A5 (1.5 nM, open triangles) on the dependence of H_2O_2 release rate on oxygen concentration in the presence of 1 μM rotenone (c), 1 μM rotenone and 25 nM uncoupler SF 6847 (d), or 1 μM rotenone and 2 μM complex III inhibitor myxothiazol (e). At least five different isolations of mitochondria were used and 5–6 traces for each experimental condition were averaged (n = 5–6). Fit parameters of Equation 1 are shown on the graphs. Concentration of glycerol 3-phosphate was 40 mM.

complex I *in vitro* (5–200 μM [O_2]) (Vinogradov and Grivennikova 2005; Kussmaul and Hirst 2006).

The hyperbolic dependence shown in liver mitochondria assayed with Amplex Red (Hoffman *et al.* 2007; Hoffman and Brookes 2009) is likely because of the different enzymatic composition of the mitochondria preparations from different tissues. As demonstrated by the work of Miwa *et al.* (Miwa *et al.* 2016), liver mitochondria possess a specific phenylmethylsulfonyl fluoride-sensitive carboxylesterase enzyme able to catalyze the deamidation of Amplex Red eventually leading to the formation of resorufin. Addition of 100 μM phenylmethylsulfonyl fluoride did not affect the H_2O_2 production rates measured in the present study, indicating that the carboxylesterase activity is not present in mouse brain mitochondria (data not shown).

As it was previously shown, the highest rate of H_2O_2 release was found in conditions of RET (Turrens and Boveris 1980; Votyakova and Reynolds 2001; Treberg *et al.* 2011), highlighting the importance of this process in pathological conditions, such as ischemia/reperfusion. Succinate levels in the brain can be elevated up to 30-fold after the periods of ischemia (Folbergrova *et al.* 1974; Benzi *et al.* 1979; Solberg *et al.* 2010; Sahni *et al.* 2017). Glycerol 3-phosphate, another substrate of RET, is also increased after brain ischemia (Nguyen *et al.* 2007). Because of the lateral oxygenation in the penumbra area and after reperfusion, ROS production by RET can overcome the capacity of matrix ROS detoxification and significantly contribute to the oxidative stress observed in ischemia/reperfusion.

Previously published results (Hinkle *et al.* 1967; Turrens and Boveris 1980; Votyakova and Reynolds 2001; Pryde and Hirst 2011; Treberg *et al.* 2011; Niatsetskaya *et al.* 2012b; Quinlan *et al.* 2013), and results of the present study (Fig. 2), show that RET-like conditions provide the highest rate of H_2O_2 release. The sensitivity of the H_2O_2 production during oxidation of succinate or glycerol 3-phosphate to rotenone and ADP identifies complex I as a major ROS contributor in these conditions. Most likely, complex I flavin is a direct electron donor for the reduction of oxygen in superoxide-generating reaction, as suggested earlier (Turrens and Boveris 1980; Liu *et al.* 2002; Kudin *et al.* 2004; Galkin and Brandt 2005; Vinogradov and Grivennikova 2005; Kussmaul and Hirst 2006; Stepanova *et al.* 2017). An oxygen molecule can approach enzyme-bound flavin only via a narrow passage formed by the NADH-binding subunit (Fiedorczuk *et al.* 2016; Zhu *et al.* 2016), so the presence of the nucleotide bound to complex I restricts the access of oxygen to flavin. Kinetic measurements (Barker *et al.* 2007; Knuuti *et al.* 2013) and atomistic dynamic simulation studies (Na *et al.* 2018) suggest that the flavin is reoxidized and electrons are transferred downstream before NAD^+ is released. During forward electron transfer, oxygen can approach the flavin only after NAD^+ is released, leaving flavin in the oxidized state, so that no ROS generation can occur. However, in conditions of RET, the entire chain of iron–sulfur clusters within the enzyme is reduced from the downstream and reduction in the flavin occurs independently of the absence or presence of nucleotide in the active center. In this scenario, flavin is in the reduced form, and the NADH-binding passage is accessible to oxygen, allowing it to interact with $FMNH_2$ to produce ROS.

The data reported here strongly reinforce this proposal and explain experimental data presented in this paper and studies by others of dual effect of rotenone-like specific inhibitors on ROS production by mitochondria oxidizing either NAD^+-depending substrates (malate and pyruvate) or succinate (Andreyev *et al.* 2005; Quinlan *et al.* 2013; Dröse *et al.* 2016). In our conditions, rotenone increases H_2O_2 release with malate and pyruvate by twofold. On the contrary, during RET, rotenone decreases H_2O_2 release by around 70 and 50% with succinate or glycerol 3-phosphate, respectively. Rotenone binds close to the quinone site of complex I and interrupts electron transfer between the terminal iron–sulfur cluster and ubiquinone (Zhu *et al.* 2016). Therefore, when malate and pyruvate are used to generate NADH, binding of rotenone increases the flavin reduction and the probability of its interaction with oxygen. In conditions of RET, rotenone prevents a reduction in flavin from the downstream, leading to decreased ROS production.

Early studies have emphasized ROS production at complex III (Boveris and Chance 1973; Turrens *et al.* 1985). Antimycin A acts as an effective inhibitor of net electron transfer by complex III by blocking the Q_i site of the enzyme. In steady-state conditions, in the presence of antimycin A, the low-potential chain becomes reduced, eliminating heme b_L as an electron acceptor. The high-potential chain remains oxidized so that the Q_o site is controlled by an excess of quinol and oxidized Rieske protein. This favors the formation of the semiquinone at the Q_o site, which can donate one electron to molecular oxygen (Ksenzenko *et al.* 1983, 1984; Crofts *et al.* 1999; Swierczek *et al.* 2010) (see also (Dröse and Brandt 2008) for a review). Without the inhibitor, the contribution of complex III to the mitochondrial ROS generation is not significant. However, the production of ROS from complex III could play a role in pathological scenarios, ranging from hereditary to acquired defects of this enzyme (Rana *et al.* 2000; Borek *et al.* 2015).

Here, we find that addition of antimycin A drastically changes the linear oxygen dependence of H_2O_2 release observed in the absence of inhibitors or in the presence of rotenone. After addition of antimycin A, the linear relationship is transformed to a more complex function which can be described as the superposition of linear and hyperbolic terms.

For the forward electron transfer (malate and pyruvate), the linear term quantitatively corresponds to the dependence in the presence of rotenone since both inhibitors block electron transfer from substrates of NAD-dependent dehydrogenases downstream. In the presence of either antimycin A or rotenone, complex I redox centers are maximally reduced; therefore, antimycin A should induce "rotenone"-like H_2O_2 release in the complex I.

When antimycin A is present during succinate oxidation, the linear component is close to state 3 respiration. Based on the slope values, the linear contribution is, probably, provided by complex II operating at diminished proton-motive force (e.g., state 3 respiration). This is consistent with the fact that inhibition of complex III by antimycin A would inevitably lead to the collapse of the proton-motive force.

When mitochondria are oxidizing glycerol 3-phosphate, the linear component has an oxygen dependence slope of 2.2 pmol H_2O_2/min/mg protein per μM [O_2] (Fig. 3c). This dependence can be because of the combined activities of GPDH (Kwong and Sohal 1998; Miwa *et al.* 2003; Tretter *et al.* 2007) and complex II (McLennan and Degli Esposti 2000; Quinlan *et al.* 2012; Siebels and Drose 2013; Grivennikova *et al.* 2017).

The hyperbolic component of oxygen dependence originating in complex III in the presence of antimycin A can be characterized by an apparent K_m for oxygen in the range of 5–12 μM, depending on the substrate used. The most straightforward explanation for the hyperbolic dependence is that one-electron reduction in O_2 at the Q_o site of complex III requires a specific site for oxygen binding that can be characterized with an apparent value of K_m. However, the Q_o site is located in the hydrophobic phase, with a wide opening at the distal part allowing for interactions with the Rieske iron–sulfur protein in the water phase (Crofts *et al.* 1999).

Since the oxygen molecule is also hydrophobic and the reaction of oxygen with semiquinone is a rapid process (Valgimigli *et al.* 2008), it is unlikely that the oxygen needs to bind to be reduced by the Q_o semiquinone. Furthermore, the K_m for oxygen had different values with different substrates and it is unlikely that this reflects the existence of different oxygen-binding sites for different substrates. Probably, the redox poise of the quinone pool upstream complex III provided by different substrates affects the value of K_m.

The reactions' rate of ROS production (v_{ROS}) from a reduced center is a second-order reaction given by:

$$v_{ROS} = \kappa \times [R] \times [O_2] \quad (3)$$

where κ is the rate constant, [R] is the concentration of the reduced species-donating electrons to O_2 (electron leakage), and $[O_2]$ is the oxygen concentration. In respiring mitochondria, the instantaneous flux via a redox center is much larger than the rate of electron leakage to oxygen with ROS formation. Therefore, the low rate of electron transfer from R to oxygen relative to the instantaneous flux will not affect the concentration of the reduced species and the rate of ROS production will be linear with oxygen concentration. In contrast, if the rate of generation of the reduced species is slow compared to the rate it reacts with oxygen, then there will be competition between the two processes and [R] will decrease at high oxygen concentrations leading to a hyperbolic relationship, as seen with antimycin. When complex III is inhibited with antimycin, the normal electron bifurcation cannot occur and the concentration of semiquinone at the Q_o center depends on the equilibrium between the semiquinone and quinol couple at the Q_o center and the redox potential of the cytochrome *c* pool. This process is not part of the normal turnover of the enzyme and so may be slow compared with the rate of electron leakage. Therefore, the ROS release from complex III in the presence of antimycin A may be explained by the effect of oxygen concentration on the semiquinone concentration at Q_o, which then participates in ROS generation. However, the exact mechanism by which antimycin induces a hyperbolic dependence of ROS production on oxygen concentration is not clear.

Finally, we found that inhibition of complex II by atpenin A5 decreases the slope of oxygen dependence in mitochondria oxidizing glycerol 3-phosphate when rotenone is present. This indicates that complex II is able to participate in ROS production in these conditions, even in the absence of succinate. The contribution of complex II to overall H_2O_2 production is probably dependent on the oxidation state of the ubiquinone pool as the uncoupler, which will oxidize the pool because of the increased rate of oxidation of ubiquinol by complex III, decreases the complex II contribution (Fig. 4d) and myxothiazol, which blocks oxidation of the pool by inhibiting complex III, increases the complex II contribution (Fig 4e). Therefore, complex II can be maintained in the reduced state and contribute to ROS generation even in the absence of its substrate when quinone pool is reduced, for example, by glycerol 3-phosphate. Our data cannot address which centers generate the ROS, but two redox centers can potentially participate: the flavin adenine dinucleotide (Orr *et al.* 2012; Dröse 2013) and the [3Fe-4S] iron–sulfur center (Yankovskaya *et al.* 2003; Grivennikova *et al.* 2017). Regardless of the center which generates the ROS, the contribution of complex II to ROS production is likely to be minor in physiological conditions.

In summary, our data suggest that ROS generation by brain mitochondria depends linearly on oxygen concentration obeying the law of mass action (Guldberg and Waage 1864). The highest rates of H_2O_2 release were observed in the conditions of RET. Complex III contributes to overall ROS production only in the presence of its specific inhibitor antimycin A, and H_2O_2 release from this enzyme shows hyperbolic dependence on oxygen concentration. Another important finding of our studies is that, in brain mitochondria, complex II can contribute to ROS generation even in the absence of succinate when the quinone pool is reduced with other substrate(s).

Although the subject of the presented study was restricted to intact brain mitochondria, there is potential clinical relevance. For example, excessive use of oxygen supplementation during resuscitation was strongly associated with greater oxidative injury and poorer neurological outcome in asphyxiated piglets and rats (Koch *et al.* 2008; Solberg *et al.* 2012). In contrast, the extent of brain injury and the acuity of cerebral oxidative damage were significantly decreased in neonatal mice reoxygenated with 18% oxygen during initial hour of reperfusion (Niatsetskaya *et al.* 2012a) The very distinctive linear dependence of the H_2O_2 release from intact mitochondria on the oxygen concentration in the absence of inhibitors will be very useful in critically testing any mechanisms proposed for role of mitochondria in hypoxic tissue response.

Acknowledgments and conflict of interest disclosure

We thank Prof. Ulrich Brandt and Prof. Peter Rich for valuable discussion and Prof. Volker Zickermann for critical reading of the manuscript. We are grateful to Anna Bunin for help in the preparation of this manuscript. The author(s) declared no potential conflicts of interest with respect to the research, authorship, and/or publication of this article. This study was supported by MRC grant MR/L007339/1 (A.G.) and by NIH grants NS-100850 (V.T.) and NS-095692 (G.M.). The authors declare no conflict of interest.

All experiments were conducted in compliance with the ARRIVE guidelines.

Author contributions

AS involved in data acquisition, analysis, data interpretation, statistical computation, and critical revision of the article; CK

involved in setting up and programming of fluorescent module and critical revision of the article; GM and VT analyzed the data and critically revised the article; RS involved in data analysis, interpretation, and critical revision of the article; AG supervised and involved in the study concept, data acquisition, data analysis, data interpretation, drafting the article, and critical revision of the article and gave the final approval.

Open science badges

This article has received a badge for *Open Materials* because it provided all relevant information to reproduce the study in the manuscript. The complete Open Science Disclosure form for this article can be found at the end of the article. More information about the Open Practices badges can be found at https://cos.io/our-services/open-science-badges/.

Supporting information

Additional supporting information may be found online in the Supporting Information section at the end of the article.

Figure S1. Dependence of H_2O_2 release rate on the oxygen concentration for oxidation of 2 mM malate 5 mM pyruvate. H_2O_2 release during non-phosphorylating (left) and phosphorylating, state 3 (middle) respiration and in the presence of rotenone (right) was measured at different [O_2] as detailed in the Materials and Methods section. Here and below all fitting parameters calculated using four different methods are shown in the table.

Figure S2. Dependence of H_2O_2 release rate on the oxygen concentration for oxidation of 5 mM succinate and 1 mM glutamate.

Figure S3. Dependence of H_2O_2 release rate on the oxygen concentration for oxidation of 40mM glycerol 3-phosphate.

Figure S4. Dependence of H_2O_2 release rate on the oxygen concentration in the presence of antimycin A.

Figure S5. Respiration and H_2O_2 release by mitochondria oxidizing glycerol 3-phosphate in the presence of rotenone.

References

Andreyev A. Y., Kushnareva Y. E. and Starkov A. A. (2005) Mitochondrial metabolism of reactive oxygen species. *Biochemistry (Mosc.)* **70**, 200–214.

Andreyev A. Y., Kushnareva Y. E., Murphy A. N. and Starkov A. A. (2015) Mitochondrial ROS metabolism: 10 Years later. *Biochemistry (Mosc.)* **80**, 517–531.

Barker C. D., Reda T. and Hirst J. (2007) The flavoprotein subcomplex of complex I (NADH:ubiquinone oxidoreductase) from bovine heart mitochondria: insights into the mechanisms of NADH oxidation and NAD^+ reduction from protein film voltammetry. *Biochemistry* **46**, 3454–3464.

Benzi G., Arrigoni E., Marzatico F. and Villa R. F. (1979) Influence of some biological pyrimidines on the succinate cycle during and after cerebral ischemia. *Biochem. Pharmacol.* **28**, 2545–2550.

Borek A., Kuleta P., Ekiert R., Pietras R., Sarewicz M. and Osyczka A. (2015) Mitochondrial disease-related mutation G167P in cytochrome b of rhodobacter capsulatus Cytochrome bc1 (S151P in Human) affects the equilibrium distribution of [2Fe-2S] cluster and generation of superoxide. *J. Biol. Chem.* **290**, 23781–23792.

Boveris A. and Chance B. (1973) The mitochondrial generation of hydrogen peroxide. General properties and effect of hyperbaric oxygen. *Biochem. J.* **134**, 707–716.

Boveris A., Oshino N. and Chance B. (1972) The cellular production of hydrogen peroxide. *Biochem. J.* **128**, 617–630.

Crofts A. R., Guergova-Kuras M., Huang L., Kuras R., Zhang Z. and Berry E. A. (1999) Mechanism of ubiquinol oxidation by the bc_1 complex: role of the iron sulfur protein and its mobility. *Biochemistry* **38**, 15791–15806.

D'Autreaux B. and Toledano M. B. (2007) ROS as signalling molecules: mechanisms that generate specificity in ROS homeostasis. *Nat. Rev. Mol. Cell Biol.* **8**, 813–824.

Dröse S. (2013) Differential effects of complex II on mitochondrial ROS production and their relation to cardioprotective pre- and postconditioning. *Biochim. Biophys. Acta* **1827**, 578–587.

Dröse S. and Brandt U. (2008) The mechanism of mitochondrial superoxide production by the cytochrome bc_1 complex. *J. Biol. Chem.* **283**, 21649–21654.

Dröse S., Stepanova A. and Galkin A. (2016) Ischemic A/D transition of mitochondrial complex I and its role in ROS generation. *Biochim. Biophys. Acta* **1857**, 946–957.

Fiedorczuk K., Letts J. A., Degliesposti G., Kaszuba K., Skehel M. and Sazanov L. A. (2016) Atomic structure of the entire mammalian mitochondrial complex I. *Nature* **537**, 644–648.

Folbergrova J., Ljunggren B., Norberg K. and Siesjo B. K. (1974) Influence of complete ischemia on glycolytic metabolites, citric acid cycle intermediates, and associated amino acids in the rat cerebral cortex. *Brain Res.* **80**, 265–279.

Galkin A. and Brandt U. (2005) Superoxide radical formation by pure complex I (NADH:ubiquinone oxidoreductase) from *Yarrowia lipolytica*. *J. Biol. Chem.* **280**, 30129–30135.

Grivennikova V. G., Kozlovsky V. S. and Vinogradov A. D. (2017) Respiratory complex II: ROS production and the kinetics of ubiquinone reduction. *Biochim. Biophys. Acta* **1858**, 109–117.

Guldberg C. M. and Waage P. (1864) Studier over affiniteten. *Forhandelinger: Videnskabs-Selskabet i Christiana*, 35–45.

Hinkle P. C., Butow R. A., Racker E. and Chance B. (1967) Partial resolution of the enzymes catalyzing oxidative phosphorylation. XV. Reverse electron transfer in the flavin-cytochrome beta region of the respiratory chain of beef heart submitochondrial particles. *J. Biol. Chem.* **242**, 5169–5173.

Hoffman D. L. and Brookes P. S. (2009) Oxygen sensitivity of mitochondrial reactive oxygen species generation depends on metabolic conditions. *J. Biol. Chem.* **284**, 16236–16245.

Hoffman D. L., Salter J. D. and Brookes P. S. (2007) Response of mitochondrial reactive oxygen species generation to steady-state oxygen tension: implications for hypoxic cell signaling. *Am. J. Physiol. Heart Circ. Physiol.* **292**, H101–H108.

Horsefield R., Yankovskaya V., Sexton G., Whittingham W., Shiomi K., Omura S., Byrne B., Cecchini G. and Iwata S. (2006) Structural and computational analysis of the quinone-binding site of complex II (succinate-ubiquinone oxidoreductase): a mechanism of electron transfer and proton conduction during ubiquinone reduction. *J. Biol. Chem.* **281**, 7309–7316.

Kalogeris T., Bao Y. and Korthuis R. J. (2014) Mitochondrial reactive oxygen species: a double edged sword in ischemia/reperfusion vs preconditioning. *Redox. Biol.* **2**, 702–714.

Kilkenny C., Browne W. J., Cuthill I. C., Emerson M. and Altman D. G. (2010) Improving bioscience research reporting: the ARRIVE guidelines for reporting animal research. *PLoS Biol.* **8**, e1000412.

Knuuti J., Belevich G., Sharma V., Bloch D. A. and Verkhovskaya M. (2013) A single amino acid residue controls ROS production in the

respiratory complex I from *Escherichia coli*. *Mol. Microbiol.* **90**, 1190–1200.

Koch J. D., Miles D. K., Gilley J. A., Yang C. P. and Kernie S. G. (2008) Brief exposure to hyperoxia depletes the glial progenitor pool and impairs functional recovery after hypoxic-ischemic brain injury. *J. Cereb. Blood Flow Metab.* **28**, 1294–1306.

Ksenzenko M., Konstantinov A. A., Khomutov G. B., Tikhonov A. N. and Ruuge E. K. (1983) Effect of electron transfer inhibitors on superoxide generation in the cytochrome bc1 site of the mitochondrial respiratory chain. *FEBS Lett.* **155**, 19–24.

Ksenzenko M., Konstantinov A. A., Khomutov G. B., Tikhonov A. N. and Ruuge E. K. (1984) Relationships between the effects of redox potential, alpha-thenoyltrifluoroacetone and malonate on $O_2^{\cdot -}$ and H_2O_2 generation by submitochondrial particles in the presence of succinate and antimycin. *FEBS Lett.* **175**, 105–108.

Kudin A. P., Bimpong-Buta N. Y., Vielhaber S., Elger C. E. and Kunz W. S. (2004) Characterization of superoxide-producing sites in isolated brain mitochondria. *J. Biol. Chem.* **279**, 4127–4135.

Kussmaul L. and Hirst J. (2006) The mechanism of superoxide production by NADH:ubiquinone oxidoreductase (complex I) from bovine heart mitochondria. *Proc. Natl Acad. Sci. USA* **103**, 7607–7612.

Kwong L. K. and Sohal R. S. (1998) Substrate and site specificity of hydrogen peroxide generation in mouse mitochondria. *Arch. Biochem. Biophys.* **350**, 118–126.

Liu Y., Fiskum G. and Schubert D. (2002) Generation of reactive oxygen species by the mitochondrial electron transport chain. *J. Neurochem.* **80**, 780–787.

Loschen G., Azzi A., Richter C. and Flohe L. (1974) Superoxide radicals as precursors of mitochondrial hydrogen peroxide. *FEBS Lett.* **42**, 68–72.

Lust W. D., Taylor C., Pundik S., Selman W. R. and Ratcheson R. A. (2002) Ischemic cell death: dynamics of delayed secondary energy failure during reperfusion following focal ischemia. *Metab. Brain Dis.* **17**, 113–121.

McLennan H. R. and Degli Esposti M. (2000) The contribution of mitochondrial respiratory complexes to the production of reactive oxygen species. *J. Bioenerg. Biomembr.* **32**, 153–162.

Miwa S., St-Pierre J., Partridge L. and Brand M. D. (2003) Superoxide and hydrogen peroxide production by Drosophila mitochondria. *Free Radic. Biol. Med.* **35**, 938–948.

Miwa S., Treumann A., Bell A., Vistoli G., Nelson G., Hay S. and von Zglinicki T. (2016) Carboxylesterase converts Amplex red to resorufin: Implications for mitochondrial H2O2 release assays. *Free Radic. Biol. Med.* **90**, 173–183.

Miyadera H., Shiomi K., Ui H. *et al.* (2003) Atpenins, potent and specific inhibitors of mitochondrial complex II (succinate-ubiquinone oxidoreductase). *Proc. Natl Acad. Sci. USA* **100**, 473–477.

Murphy M. P. (2009) How mitochondria produce reactive oxygen species. *Biochem. J.* **417**, 1–13.

Na S., Jurkovic S., Friedrich T. and Koslowski T. (2018) Charge transfer through a fragment of the respiratory complex I and its regulation: an atomistic simulation approach. *Phys. Chem. Chem. Phys.* **20**, 20023–20032.

Nguyen N. H., Gonzalez S. V. and Hassel B. (2007) Formation of glycerol from glucose in rat brain and cultured brain cells. Augmentation with kainate or ischemia. *J. Neurochem.* **101**, 1694–1700.

Niatsetskaya Z. V., Charlagorla P., Matsukevich D. A., Sosunov S. A., Mayurasakorn K., Ratner V. I., Polin R. A., Starkov A. A. and Ten V. S. (2012a) Mild hypoxemia during initial reperfusion alleviates the severity of secondary energy failure and protects brain in neonatal mice with hypoxic-ischemic injury. *J. Cereb. Blood Flow Metab.* **32**, 232–241.

Niatsetskaya Z. V., Sosunov S. A., Matsiukevich D., Utkina-Sosunova I. V., Ratner V. I., Starkov A. A. and Ten V. S. (2012b) The oxygen free radicals originating from mitochondrial complex I contribute to oxidative brain injury following hypoxia-ischemia in neonatal mice. *J. Neurosci.* **32**, 3235–3244.

Orr A. L., Quinlan C. L., Perevoshchikova I. V. and Brand M. D. (2012) A refined analysis of superoxide production by mitochondrial sn-glycerol 3-phosphate dehydrogenase. *J. Biol. Chem.* **287**, 42921–42935.

Oshino N., Jamieson D. and Chance B. (1975) The properties of hydrogen peroxide production under hyperoxic and hypoxic conditions of perfused rat liver. *Biochem. J.* **146**, 53–65.

Patole M. S., Swaroop A. and Ramasarma T. (1986) Generation of H_2O_2 in brain mitochondria. *J. Neurochem.* **47**, 1–8.

Pryde K. R. and Hirst J. (2011) Superoxide is produced by the reduced flavin in mitochondrial complex I: a single, unified mechanism that applies during both forward and reverse electron transfer. *J. Biol. Chem.* **286**, 18056–18065.

Quinlan C. L., Orr A. L., Perevoshchikova I. V., Treberg J. R., Ackrell B. A. and Brand M. D. (2012) Mitochondrial complex II can generate reactive oxygen species at high rates in both the forward and reverse reactions. *J. Biol. Chem.* **287**, 27255–27264.

Quinlan C. L., Perevoshchikova I. V., Hey-Mogensen M., Orr A. L. and Brand M. D. (2013) Sites of reactive oxygen species generation by mitochondria oxidizing different substrates. *Redox. Biol.* **1**, 304–312.

Rana M., de Coo I., Diaz F., Smeets H. and Moraes C. T. (2000) An out-of-frame cytochrome b gene deletion from a patient with parkinsonism is associated with impaired complex III assembly and an increase in free radical production. *Ann. Neurol.* **48**, 774–781.

Rosenthal R. E., Hamud F., Fiskum G., Varghese P. J. and Sharpe S. (1987) Cerebral ischemia and reperfusion: prevention of brain mitochondrial injury by lidoflazine. *J. Cereb. Blood Flow Metab.* **7**, 752–758.

Sahni P. V., Zhang J., Sosunov S., Galkin A., Niatsetskaya Z., Starkov A., Brookes P. S. and Ten V. S. (2017) Krebs cycle metabolites and preferential succinate oxidation following neonatal hypoxic-ischemic brain injury in mice. *Pediatr. Res.* **83**, 491–497.

Schieber M. and Chandel N. S. (2014) ROS function in redox signaling and oxidative stress. *Curr. Biol.* **24**, R453–R462.

Siebels I. and Drose S. (2013) Q-site inhibitor induced ROS production of mitochondrial complex II is attenuated by TCA cycle dicarboxylates. *Biochim. Biophys. Acta* **1827**, 1156–1164.

Solberg R., Enot D., Deigner H. P., Koal T., Scholl-Burgi S., Saugstad O. D. and Keller M. (2010) Metabolomic analyses of plasma reveals new insights into asphyxia and resuscitation in pigs. *PLoS ONE* **5**, e9606.

Solberg R., Longini M., Proietti F., Vezzosi P., Saugstad O. D. and Buonocore G. (2012) Resuscitation with supplementary oxygen induces oxidative injury in the cerebral cortex. *Free Radic. Biol. Med.* **53**, 1061–1067.

Starkov A. A., Andreyev A. Y., Zhang S. F., Starkova N. N., Korneeva M., Syromyatnikov M. and Popov V. N. (2014) Scavenging of H_2O_2 by mouse brain mitochondria. *J. Bioenerg. Biomembr.* **46**, 471–477.

Stepanova A., Kahl A., Konrad C., Ten V., Starkov A. S. and Galkin A. (2017) Reverse electron transfer results in a loss of flavin from mitochondrial complex I: potential mechanism for brain ischemia reperfusion injury. *J. Cereb. Blood Flow Metab.* **37**, 3649–3658.

Swierczek M., Cieluch E., Sarewicz M., Borek A., Moser C. C., Dutton P. L. and Osyczka A. (2010) An electronic bus bar lies in the core of cytochrome bc1. *Science* **329**, 451–454.

Treberg J. R., Quinlan C. L. and Brand M. D. (2011) Evidence for two sites of superoxide production by mitochondrial NADH-

ubiquinone oxidoreductase (complex I). *J. Biol. Chem.* **286**, 27103–27110.

Tretter L., Takacs K., Hegedus V. and Adam-Vizi V. (2007) Characteristics of alpha-glycerophosphate-evoked H_2O_2 generation in brain mitochondria. *J. Neurochem.* **100**, 650–663.

Turrens J. F. and Boveris A. (1980) Generation of superoxide anion by the NADH dehydrogenase of bovine heart mitochondria. *Biochem J* **191**, 421–427.

Turrens J. F., Freeman B. A. and Crapo J. D. (1982a) Hyperoxia increases H_2O_2 release by lung mitochondria and microsomes. *Arch. Biochem. Biophys.* **217**, 411–421.

Turrens J. F., Freeman B. A., Levitt J. G. and Crapo J. D. (1982b) The effect of hyperoxia on superoxide production by lung submitochondrial particles. *Arch. Biochem. Biophys.* **217**, 401–410.

Turrens J. F., Alexandre A. and Lehninger A. L. (1985) Ubisemiquinone is the electron donor for superoxide formation by complex III of heart mitochondria. *Arch. Biochem. Biophys.* **237**, 408–414.

Valgimigli L., Amorati R., Fumo M. G., DiLabio G. A., Pedulli G. F., Ingold K. U. and Pratt D. A. (2008) The unusual reaction of semiquinone radicals with molecular oxygen. *J. Org. Chem.* **73**, 1830–1841.

Vinogradov A. D. and Grivennikova V. G. (2005) Generation of superoxide-radical by the NADH:ubiquinone oxidoreductase of heart mitochondria. *Biochemistry (Mosc.)* **70**, 120–127.

Votyakova T. V. and Reynolds I. J. (2001) $\Delta\Psi_m$-dependent and -independent production of reactive oxygen species by rat brain mitochondria. *J. Neurochem.* **79**, 266–277.

Yankovskaya V., Horsefield R., Tornroth S., Luna-Chavez C., Leger C., Byrne B., Cecchini G. and Iwata S. (2003) Architecture of succinate dehydrogenase and reactive oxygen species generation. *Science* **299**, 700–704.

Zhu J., Vinothkumar K. R. and Hirst J. (2016) Structure of mammalian respiratory complex I. *Nature* **536**, 354–358.

Open Practices Disclosure

Manuscript Title: The dependence of brain mitochondria reactive oxygen species production on oxygen level is linear, except when inhibited by antimycin A

Corresponding Author: Alexander Galkin

Articles accepted to *Journal of Neurochemistry* after 01.2018 are eligible to earn badges that recognize open scientific practices: publicly available data, material, or preregistered research plans. Please read more about the badges in our *author guidelines and Open Science Badges page*, and you can also find information on the Open Science Framework wiki.

[X] Please check this box if you are interested in participating.

To apply for one or more badges acknowledging open practices, please check the box(es) corresponding to the desired badge(s) below and provide the information requested in the relevant sections. To qualify for a badge, you must provide a URL, doi, or other permanent path for accessing the specified information in a public, open-access repository. **Qualifying public, open-access repositories are committed to preserving data, materials, and/or registered analysis plans and keeping them publicly accessible via the web in perpetuity.** Examples include the Open Science Framework (OSF) and the various Dataverse networks. Hundreds of other qualifying data/materials repositories are listed at http://re3data.org/. Preregistration of an analysis plan must take place via a publicly accessible registry system (e.g., OSF, ClinicalTrials.gov or other trial registries in the WHO Registry Network, institutional registration systems). **Personal websites and most departmental websites do not qualify as repositories.**

Authors who wish to publicly post third-party material in their data, materials, or preregistration plan must have the proper authority or permission agreement in order to do so.

There are circumstances in which it is not possible or advisable to share any or all data, materials, or a research plan publicly. For example, there are cases in which sharing participants' data could violate confidentiality. If you would like your article to include an explanation of such circumstances and/or provide links to any data or materials you have made available—even if not under conditions eligible to earn a badge—you may write an alternative note that will be published in a note in the article**.** Please check this box if you would like your article to include an alternative note and provide the text of the note below:

[] Alternative note:

[] Open Data Badge

1. Provide the URL, doi, or other **permanent path** for accessing the data in a **public, open-access repository**:

[] Confirm that there is sufficient information for an independent researcher to reproduce **all of the reported results**, including codebook if relevant.

[] Confirm that you have registered the uploaded files so that they are **time stamped** and cannot be age.

[X] Open Materials Badge

1. Provide the URL, doi, or other **permanent path** for accessing the materials in a **public, open-access repository**: all relevant information is provided in the manuscript and custom-made materials will be provided upon reasonable request.

[X] Confirm that there is sufficient information for an independent researcher to reproduce **all of the reported methodology**.

[] Confirm that you have registered the uploaded files so that they are **time stamped** and cannot be age.

[] Preregistered Badge

1. Provide the URL, doi, or other **permanent path** to the registration in a **public, open-access repository***:

2. Was the analysis plan registered prior to examination of the data or observing the outcomes? If no, explain.**

3. Were there additional registrations for the study other than the one reported? If yes, provide links and explain.*

*No badge will be awarded if (1) is not provided, **or** if (3) is answered “yes” without strong justification

**If the answer to (2) is “no,” the notation DE (Data Exist) will be added to the badge, indicating that registration postdates realization of the outcomes but predates analysis.

By signing below, authors affirm that the above information is accurate and complete, that any third-party material has been reproduced or otherwise made available only with the permission of the original author or copyright holder, and that publicly posted data do not contain information that would allow individuals to be identified without consent.

Date: __**31/10/2018**_____

Name: ___**Alexander Galkin**_____

Signature: _____